

AN UPPER LIMIT TO PHOTONS FROM FIRST DATA TAKEN BY THE PIERRE AUGER OBSERVATORY

Markus Risse^a for the Pierre Auger Collaboration^b

Forschungszentrum Karlsruhe, Institut für Kernphysik, 76021 Karlsruhe, Germany

Many models for ultra-high energy cosmic rays postulate exotic scenarios to explain the sources or the nature of these particles. A characteristic feature of these models is the prediction of a significant flux of photons at ultra-high energy. The Pierre Auger Observatory offers a great potential to search for such photons. We present shower observables with sensitivity to photons and the search strategy employed. An upper limit to photon primaries is derived from first Auger data. Prospects for constraining theoretical source models are discussed.

1 Introduction

The origin of ultra-high energy (UHE) cosmic rays above 10^{19} eV (= 10 EeV) is still unknown.¹ A “smoking gun” of non-acceleration (top-down) models of UHE cosmic-ray origin is the observation of UHE photons. These models (Super Heavy Dark Matter,² Topological Defects,³ Z-Bursts,⁴ ...) were invoked in particular to account for a possible continuation⁵ of the cosmic-ray flux above $E_{GZK} \sim 6 \times 10^{19}$ eV without the flux suppression expected from photo-pionproduction of nucleons on the microwave background.⁶ From considerations of QCD fragmentation,⁷ copious UHE photons are predicted to be generated as secondaries in the decay or annihilation chains of the proposed particles and interactions. Photon fractions in the cosmic-ray flux at the Earth of $\sim 10\%$ above 10 EeV and $\sim 50\%$ above 100 EeV would result.^{8,9,10,11} Based on first data registered by the Pierre Auger Observatory,¹² we present an upper limit to the fraction of UHE photons by comparing the observed air showers to calculations assuming photons as primaries. Further details of this analysis can also be found in Ref. ¹³.

Giant air shower experiments are well suited to search for UHE photons. Similar to nuclear primaries and unlike neutrino primaries, the atmospheric overburden is large enough for UHE photons to initiate a well-observable particle cascade. Certain observables in photon-induced showers are expected to show distinct differences compared to those in nuclear primary showers. This is firstly, because for nuclear primaries it takes several cascading steps until most energy is transferred to electrons and photons, while photons initiate an almost purely electromagnetic cascade. Secondly and connected to this, the high-energy processes of LPM¹⁴ and preshower^{15,16} effect strongly modify photon showers but not nuclear ones at 10-100 EeV. In particular, UHE photon showers are expected to reach their maximum at significantly larger depths, see Figure 1. In this work, we obtain a photon limit from the *direct* observation of the

^aNow at: University of Wuppertal, Department of Physics, 42097 Wuppertal, Germany; electronic address: risse@physik.uni-wuppertal.de

^bThe full author list is available at <http://www.auger.org/admin> .

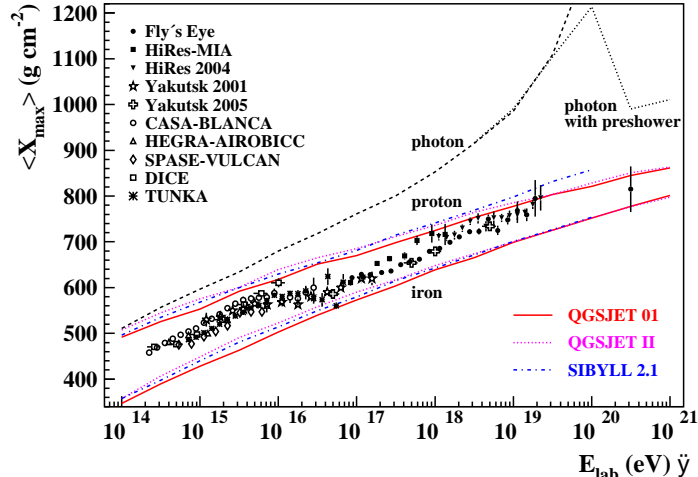


Figure 1: Average depth of shower maximum $\langle X_{\max} \rangle$ versus energy simulated for primary photons, protons and iron nuclei. Depending on the specific particle trajectory through the geomagnetic field, photons above $\sim 5 \times 10^{19}$ eV can create a preshower: as indicated by the splitting of the photon line, the average X_{\max} values then do not only depend on primary energy but also on arrival direction. For nuclear primaries, calculations for different hadronic interaction models are displayed (QGSJET 01,¹⁷ QGSJET II,¹⁸ SIBYLL 2.1¹⁹). Also shown are experimental data (for references to the experiments, see Ref. ²⁰).

shower profile with fluorescence telescopes, using the depth of shower maximum X_{\max} as the discriminating observable.

2 Data

The Auger data used in this analysis were taken with a total of 12 fluorescence telescopes situated at two different sites,²¹ during the period January 2004 to February 2006. The number of surface detector stations deployed²² grew during this period from about 150 to 950. To achieve a high accuracy in reconstructing the shower geometry, we make use of the “hybrid” detection technique, i.e. we select events observed by both the ground array and the fluorescence telescopes.²³ A detailed description of the Auger Observatory is given in.¹²

Cascading of photons in the geomagnetic field¹⁵ is simulated with the PRESHOWER code¹⁶ and shower development in air, including the LPM effect,¹⁴ is calculated with CORSIKA.²⁴ For photo-nuclear processes, we assume the extrapolation of the cross-section as given by the Particle Data Group,²⁵ and we employed QGSJET 01¹⁷ as a hadron event generator.

The reconstruction of the shower profiles^{21,26} is based on an end-to-end calibration of the fluorescence telescopes.²⁷ Monthly models for the atmospheric density profiles are used which were derived from local radio soundings.²⁸ An average aerosol model is adopted based on measurements of the local atmospheric aerosol content.²⁹ Cloud information is provided by IR monitors, positioned at the telescope stations.²⁹ Cross-checks on clouds are obtained from measurements with LIDAR systems (near the telescopes) and with a laser facility near the center of the array.^{29,30} The Cherenkov light contribution of the shower is calculated according to Ref. ³¹. An energy deposit profile is reconstructed for each event. A Gaisser-Hillas function³² is fitted to the profile to obtain the depth of shower maximum, and the calorimetric shower energy is obtained by integration. A 1% correction for missing energy assuming photon primaries³³ is applied.

The following quality cuts are applied for event selection: (i) quality of hybrid geometry: distance of closest approach of the reconstructed shower axis to the array tank with the largest signal < 1.5 km, and difference between the reconstructed shower front arrival time at this tank

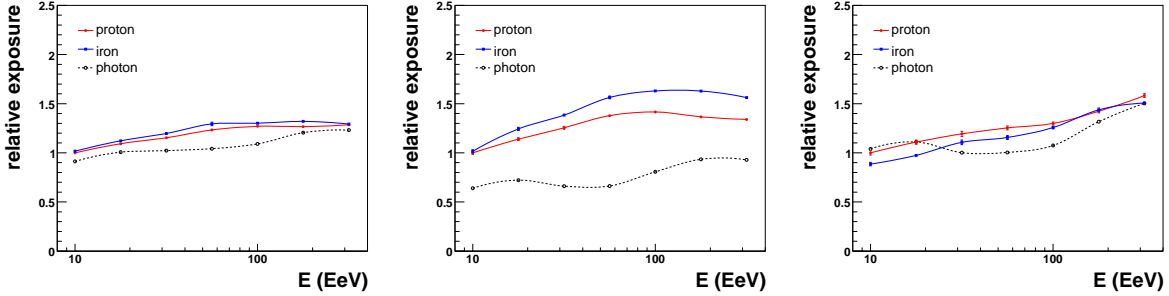


Figure 2: Relative exposures for photon, proton, and iron primaries as a function of energy after trigger (left), after quality cuts (middle) and after fiducial volume cuts are applied (right) to reduce the bias against photons. A reference value of one is adopted for proton at 10 EeV.

and the measured tank time <300 ns, (ii) number of phototubes in the fluorescence detector triggered by shower ≥ 6 , (iii) quality of Gaisser-Hillas (GH) profile fit: $\chi^2(\text{GH})$ per degree of freedom < 6 , and $\chi^2(\text{GH})/\chi^2(\text{line}) < 0.9$, where $\chi^2(\text{line})$ refers to a straight line fit, (iv) minimum viewing angle of shower direction towards the telescope $> 15^\circ$, (v) primary energy $E > 10^{19}$ eV, (vi) X_{max} observed in the field of view, (vii) cloud monitors confirm no disturbance of event observation by clouds.

Care must be taken about a possible bias of the detector acceptance against photon primaries. In Figure 2 we show the acceptance for photons and nuclear primaries at different steps of the analysis, computed using shower simulations with the CONEX code³⁴ which reproduces well the CORSIKA predictions for shower profiles. Light emission and propagation through the atmosphere and the detector response were simulated according to Ref.³⁵. As can be seen from the Figure, the acceptances are comparable for all types of primaries after trigger (left plot). However, after profile quality cuts (middle plot) the detection efficiency for photons is smaller by a factor ~ 2 than for nuclear primaries, because primary photons reach shower maximum at such large depths (of about 1000 g cm^{-2} , see Figure 1) that for a large fraction of showers the maximum is outside the field of view of the telescopes. To reduce the corresponding bias against photons, near-vertical events are excluded in the current analysis. Since the average depth of shower maximum increases with photon energy before the onset of preshower, a mild dependence of the minimum zenith angle with energy is chosen. In addition, an energy-dependent distance cut is applied to the data as the telescopes do not observe shower portions near the horizon: (i) zenith angle $> 35^\circ + g_1(E)$, with $g_1(E) = 10(\lg E/\text{eV} - 19.0)^\circ$ for $\lg E/\text{eV} \leq 19.7$ and $g_1(E) = 7^\circ$ for $\lg E/\text{eV} > 19.7$, (ii) maximum distance of telescope to shower impact point $< 24 \text{ km} + g_2(E)$, with $g_2(E) = 12(\lg E/\text{eV} - 19.0) \text{ km}$.

The acceptances after application of the fiducial volume cuts are shown in Figure 2 (right plot). The differences between photons and nuclear primaries are now significantly reduced, with the acceptances being comparable at energies 10–20 EeV. With increasing energy, the acceptance for nuclear primaries shows a modest growth, while the photon acceptance is quite flat in the investigated energy range. Comparing photons to nuclear primaries, the minimum ratio of acceptances is $\epsilon_{\text{min}} \simeq 0.80$ at energies 50–60 EeV. At even higher energies, the preshower effect becomes increasingly important, and acceptances for photons and nuclear primaries become more similar. To obtain an experimental limit to the photon fraction without relying on assumptions on energy spectra of different primaries, a correction to the photon limit is applied by conservatively adopting the minimum ratio of acceptances ϵ_{min} (a detailed derivation of the approach is given in Ref.¹³).

Applying the cuts to the data, 29 events with energies greater than 10 EeV satisfy the selection criteria. Due to the steep cosmic-ray spectrum, most events in the sample (23 out of 29) are below 20 EeV. Figure 3 (left plot) shows the longitudinal profile of an event reconstructed

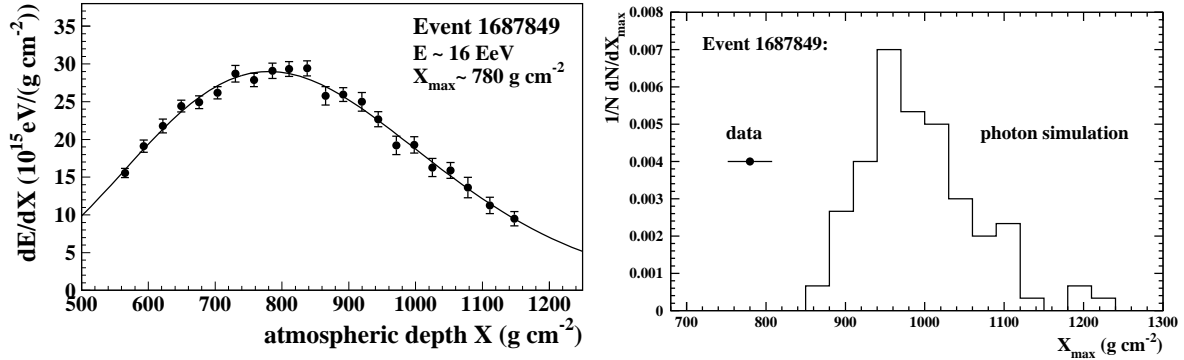


Figure 3: *Left:* example of a reconstructed longitudinal energy deposit profile (points) and the fit by a Gaisser-Hillas function (line). *Right:* X_{\max} measured in the shower shown on the left-hand side (point with error bar) compared to the X_{\max}^{γ} distribution expected for photon showers (solid line).

with 16 EeV and $X_{\max} = 780 \text{ g cm}^{-2}$. The X_{\max} values of the selected events are displayed in Figure 4. A Table summarising the main shower characteristics for all events can be found in Ref. ¹³.

The uncertainty ΔX_{\max} of the reconstructed depth of shower maximum is composed of several contributions, some of which may vary from event to event. In this work, we conservatively adopt overall estimates for the current statistical and systematic uncertainties which are applied to all selected events. These uncertainties are expected to decrease significantly in the future. However, even when adopting conservative estimates, the present analysis is not limited by the measurement uncertainties but by event statistics. This is due to the fact that shower fluctuations for photons are considerably larger than the measurement uncertainties.

Main contributions to ΔX_{\max} of 10–20 g cm^{-2} each are the uncertainties in the profile fit, in shower geometry, and in atmospheric conditions (see Table in Ref. ¹³). The current systematic uncertainty of 25% in energy reconstruction²¹ translates to a $\sim 13 \text{ g cm}^{-2}$ systematic uncertainty in the X_{\max}^{γ} values predicted from photon simulations. The uncertainty from extrapolating the photo-nuclear cross-section to high energies is estimated to $\sim 10 \text{ g cm}^{-2}$.^{36,37} Contrary to the case of nuclear primaries, uncertainties from modelling high-energy hadron interactions are much less important in primary photon showers (uncertainty of $\sim 5 \text{ g cm}^{-2}$): this is a great advantage of this type of analysis where data are compared to calculations of primary photon showers only. Adding in quadrature the individual contributions gives a statistical uncertainty $\Delta X_{\max}^{\text{stat}} \simeq 28 \text{ g cm}^{-2}$ and a systematic uncertainty $\Delta X_{\max}^{\text{syst}} \simeq 23 \text{ g cm}^{-2}$.

For each selected event, 100 showers were simulated as photon primaries. Since photon shower features can depend in a non-trivial way on arrival direction and energy, the specific event conditions were adopted for each event.

3 Results

In Figure 3 (right plot) the predictions for X_{\max}^{γ} for a photon primary are compared with the measurement of $X_{\max} = 780 \text{ g cm}^{-2}$ for the event shown in the left plot of Figure 3. With $\langle X_{\max}^{\gamma} \rangle \simeq 1000 \text{ g cm}^{-2}$, photon showers are on average expected to reach maximum at depths considerably greater than that observed for real events. Shower-to-shower fluctuations are large due to the LPM effect. For this event, the expectation for a primary photon differs by $\Delta_{\gamma} \simeq +2.9$ standard deviations from the data, where Δ_{γ} is calculated from

$$\Delta_{\gamma} = \frac{\langle X_{\max}^{\gamma} \rangle - X_{\max}}{\sqrt{(\Delta X_{\max}^{\gamma})^2 + (\Delta X_{\max}^{\text{stat}})^2}} . \quad (1)$$

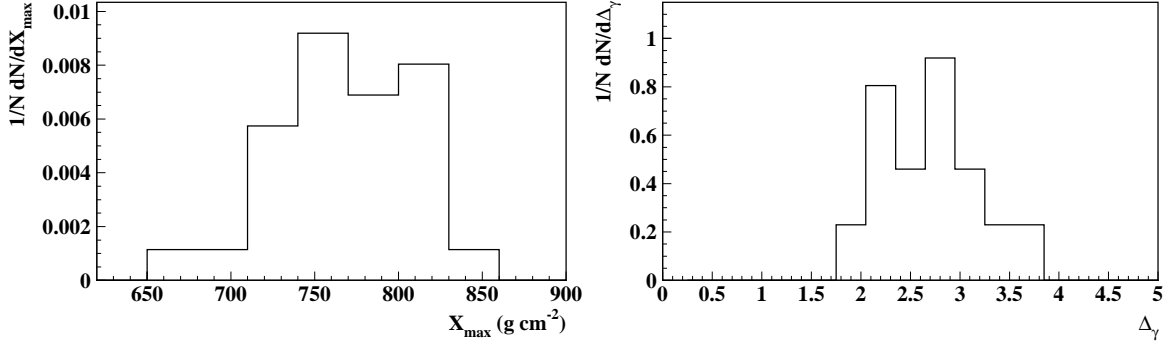


Figure 4: *Left:* Distribution of X_{\max} values of the 29 selected events. *Right:* distribution of differences Δ_γ in standard deviations between primary photon prediction and data for the 29 selected events.

For all events, the observed X_{\max} is well below the average value expected for photons. The distribution of observed X_{\max} values is shown in Figure 4 (left plot). The differences Δ_γ between photon prediction and data range from +2.0 to +3.8 standard deviations, see Figure 4 (right plot). It is extremely unlikely that all 29 events were initiated by photons (probability $\ll 10^{-10}$), so an upper limit to the fraction of cosmic-ray photons above 10 EeV can be reliably set. Due to the limited event statistics, the upper limit cannot be smaller than a certain value. For 29 events and $\epsilon_{\min} \simeq 0.80$, the minimum possible value for an upper limit to be set at a 95% confidence level is $\sim 12\%$. The theoretical limit is reached only if a photon origin is basically excluded for all events.

The calculation of the upper limit is based on the statistical method introduced in Ref. ³⁹ which is tailor-made for relatively small event samples. For each event, trial values $\chi^2 = \Delta_\gamma^2$ are calculated with Δ_γ according to Eq. (1). We distinguish between statistical and systematic uncertainties for the depths of shower maximum. The method in Ref. ³⁹ is extended to allow for a correlated shift of the observed X_{\max} values for all selected events, where the shifted value is drawn at random from a Gaussian distribution with a width $\Delta X_{\max}^{\text{sys}} = 23 \text{ g cm}^{-2}$. For the shifted data, new χ^2 values are calculated from Eq. (1). Many such “shifted” event sets are generated from the data and compared to artificial data sets using photon simulations. The chance probability $p(f_\gamma)$ is calculated to obtain artificial data sets with χ^2 values larger than observed as a function of the hypothetical primary photon fraction f_γ . Possible non-Gaussian shower fluctuations are accounted for in the method, as the probability is constructed by a Monte Carlo technique. The upper limit f_γ^{ul} , at a confidence level α , is then obtained from $p(f_\gamma \geq \epsilon_{\min} f_\gamma^{\text{ul}}) \leq 1 - \alpha$, where the factor $\epsilon_{\min} = 0.80$ accounts for the different detector acceptance for photon and nuclear primaries.

For the Auger data sample, an upper limit to the photon fraction of 16% at a confidence level of 95% is derived. In Figure 5, this upper limit is plotted together with previous experimental limits and some illustrative estimates for non-acceleration models. We have shown two different expectations for SHDM decay ^{10,11} to illustrate the sensitivity to assumptions made about the decay mode and the fragmentation, as well as the normalisation of the spectrum. The derived limit is the first one based on observing the depth of shower maximum with the fluorescence technique. The result confirms and improves previous limits above 10 EeV that were derived from surface arrays. It is worth mentioning that this improved limit is achieved with only 29 events above 10 EeV, as compared to about 50 events in the Haverah Park analysis and about 120 events in the AGASA analysis.

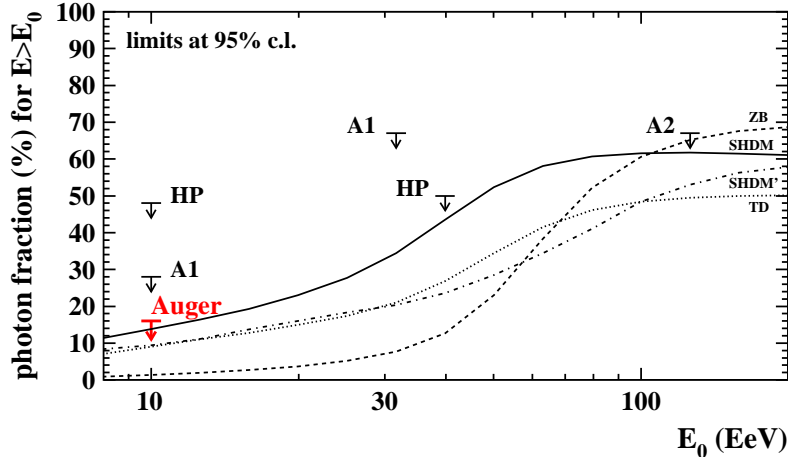


Figure 5: Upper limits (95% c.l.) to the cosmic-ray photon fraction derived in the present analysis (Auger) and obtained previously from AGASA (A1),³⁸ (A2),³⁹ and Haverah Park (HP)⁴⁰ data, compared to expectations for non-acceleration models (ZB, SHDM, TD from Ref. ¹⁰, SHDM' from Ref. ¹¹).

4 Outlook

The current analysis is limited mainly by the small number of events. The number of hybrid events will considerably increase over the next years, and much lower primary photon fractions can be tested. With a data increase of about an order of magnitude compared to the current analysis, as is expected to be reached in 2008/2009, photon fractions of $\sim 5\%$ can be tested. Moreover, the larger statistics will allow us to increase the threshold energy above 10 EeV where even larger photon fractions are predicted by most models. A comparable number of events as for the present analysis would be reached then above 30–35 EeV. An upper limit similar to the current one but at this higher energy would severely constrain non-acceleration models.

In this work, data from the surface array are used only to achieve a high precision of reconstructed shower geometry in hybrid events. A single tank was sufficient for this. However, observables registered by the surface array are also sensitive to the primary particle type and can be exploited for studies of primary photon showers.⁴¹ An example for another observable is given by the *risetime* of the shower signal in the detectors, one measure of the time spread of particles in the shower disc. For each triggered tank, we define a risetime as the time for the integrated signal to go from 10% to 50% of its total value. By interpolation between risetimes recorded by the tanks at different distances to the shower core, the risetime at 1000 m core distance is extracted after correcting for azimuthal asymmetries in the shower front. For the specific event shown in Figure 3, the measured risetime is compared to the simulated distribution in Figure 6. The observed risetime does not agree well with the predictions for primary photons. In future photon analyses, the independent information on the primary particle from the Auger ground array and fluorescence telescope data can be used to cross-check each other. Combining the different shower observables will further improve the discrimination power to photons.

If only surface detector data are used, event statistics are increased by about an order of magnitude. However, care must be taken about a possible bias against photons in an array-only analysis because of the different detector acceptance for photon and nuclear primaries. Also, compared to the near-calorimetric energy determination in the fluorescence technique, the energy estimated from array data shows a stronger dependence on the primary type and is more strongly affected by shower fluctuations. These issues are under current investigation.

It is planned to complement the southern site of the Auger Observatory by a northern one in Colorado. This can substantially improve the sensitivity to UHE photons. It is then

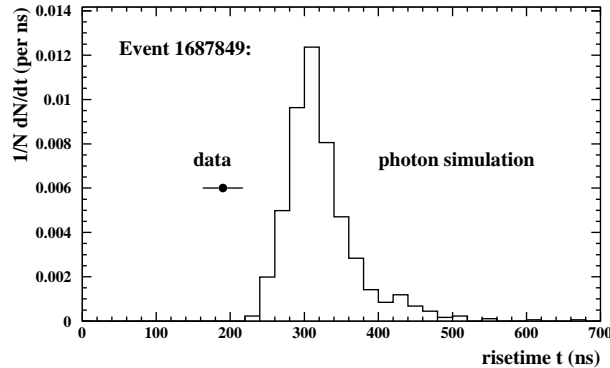


Figure 6: Example of risetime measured in an individual shower, same as in Figure 3 (point with error bar) compared to the risetime distribution expected for photon showers (solid line).

important to note that UHE photons are expected to be produced during propagation even if the sources emit nucleons only, resulting in a “guaranteed” flux of UHE photons.¹⁰ Detection of these photons would be a major step forward for investigating sources and interactions at UHE.

Comparing the northern and southern Auger sites, differences in the expected preshower features exist.⁴² Due to the stronger (factor ~ 2) magnetic field, the preshower process starts at smaller energies at the northern site. The “sky pattern” for preshowering (probability of geomagnetic pair production for a given energy as a function of the arrival direction) is shifted according to the different pointing of the local magnetic field lines. Interestingly, values of $\sim 100\%$ preshower probability are reached for the full sky at higher energies in Colorado (despite the stronger magnetic field on ground), which is connected to the field lines being less curved with distance from the ground. These differences may be exploited to search for UHE photons or, in particular, to obtain independent proof of a possible photon signal detected at one site.

Acknowledgments

It is a pleasure to thank the organizers of the *Rencontres du Vietnam* for their invitation and for a very pleasant and informative conference atmosphere. The author is grateful to K.-H. Kampert for helpful comments on the manuscript. Partial support from the Helmholtz VIHKOS Institute and from the German Ministry for Education and Research is kindly acknowledged.

References

1. M. Nagano, A.A. Watson, Rev. Mod. Phys. **72**, 689 (2000); “*Ultimate energy particles in the Universe*”, eds. M. Boratav and G. Sigl, C.R. Physique **5**, Elsevier, Paris (2004); J. Cronin, Nucl. Phys. B, Proc. Suppl. **138** (2005), 465.
2. V. Berezhinsky, M. Kachelrieß, A. Vilenkin, Phys. Rev. Lett. **79**, 4302 (1997); M. Birkel, S. Sarkar, Astropart. Phys. **9**, 297 (1998).
3. C.T. Hill, Nucl. Phys. **B224**, 469 (1983); M.B. Hindmarsh, T.W.B. Kibble, Rep. Prog. Phys. **58**, 477 (1995).
4. T.J. Weiler, Phys. Rev. Lett. **49**, 234 (1982); T.J. Weiler, Astropart. Phys. **11**, 303 (1999); D. Fargion, B. Mele, A. Salis, Astrophys. J. **517**, 725 (1999).
5. M. Takeda *et al.*, Astropart. Phys. **19**, 447 (2003).
6. K. Greisen, Phys. Rev. Lett. **16**, 748 (1966); G.T. Zatsepin, V.A. Kuzmin, JETP Lett. **4** 78 (1966).
7. Z. Fodor, S.D. Katz, Phys. Rev. Lett. **86**, 3224 (2001); S. Sarkar, R. Toldra,

- Nucl. Phys. **B621**, 495 (2002); C. Barbot, M. Drees, *Astropart. Phys.* **20**, 5 (2003); R. Aloisio, V. Berezhinsky, M. Kachelrieß, *Phys. Rev.* **D69**, 094023 (2004).
8. P. Bhattacharjee, G. Sigl, *Phys. Rep.* **327**, 109 (2000).
 9. S. Sarkar, *Acta Phys. Polon.* **B35**, 351 (2004).
 10. G. Gelmini, O.E. Kalashev, D.V. Semikoz, [arXiv:astro-ph/0506128].
 11. J. Ellis, V. Mayes, D.V. Nanopoulos, *Phys. Rev. D* **74**, 115003 (2006).
 12. J. Abraham *et al.*, Pierre Auger Collaboration, *Nucl. Instrum. Meth.* **A 523**, 50 (2004).
 13. J. Abraham *et al.*, Pierre Auger Collaboration, *An upper limit to the photon fraction in cosmic rays above 10^{19} eV from the Pierre Auger Observatory*, *Astropart. Phys.* (2006), in press, doi:10.1016/j.astropartphys.2006.10.004, [arXiv:astro-ph/0606619].
 14. L.D. Landau, I.Ya. Pomeranchuk, *Dokl. Akad. Nauk SSSR* **92**, 535 & 735 (1953); A.B. Migdal, *Phys. Rev.* **103**, 1811 (1956).
 15. T. Erber, *Rev. Mod. Phys.* **38**, 626 (1966); B. McBreen, C.J. Lambert, *Phys. Rev. D* **24**, 2536 (1981); T. Stanev, H.P. Vankov, *Phys. Rev. D* **55**, 1365 (1997).
 16. P. Homola *et al.*, *Comp. Phys. Comm.* **173**, 71 (2005).
 17. N.N. Kalmykov, S.S. Ostapchenko, A.I. Pavlov, *Nucl. Phys. B (Proc. Suppl.)* **52B**, 17 (1997).
 18. S. Ostapchenko, *Nucl. Phys. B (Proc. Suppl.)* **151**, 143 (2006).
 19. R. Engel, T.K. Gaisser, P. Lipari, T. Stanev, *Proc. 26th ICRC*, Salt Lake City, 415 (1999).
 20. J. Knapp *et al.*, *Astropart. Phys.* **19**, 77 (2003).
 21. J. Bellido [Pierre Auger Collaboration], *Proc. 29th ICRC*, Pune, **7**, 13 (2005), [arXiv:astro-ph/0508389].
 22. X. Bertou [Pierre Auger Collaboration], *Proc. 29th ICRC*, Pune, **7**, 1 (2005), [arXiv:astro-ph/0508466].
 23. M.A. Mostafá [Pierre Auger Collaboration], *Proc. 29th ICRC*, Pune, **7**, 369 (2005).
 24. D. Heck *et al.*, *Reports FZKA 6019 & 6097*, Forschungszentrum Karlsruhe (1998).
 25. S. Eidelmann *et al.*, Particle Data Group, *Phys. Lett.* **B592**, 1 (2004).
 26. T. Paul *et al.* [Pierre Auger Collaboration], *Proc. 29th ICRC*, Pune, **8**, 343 (2005).
 27. A.C. Rovero *et al.* [Pierre Auger Collaboration], *Proc. 29th ICRC*, Pune, **8**, 5 (2005), [arXiv:astro-ph/0507347].
 28. B. Keilhauer *et al.* [Pierre Auger Collaboration], *Proc. 29th ICRC*, Pune, **7**, 123 (2005), [arXiv:astro-ph/0507275].
 29. M. Roberts *et al.* [Pierre Auger Collaboration], *Proc. 29th ICRC*, Pune, **8**, 347 (2005).
 30. M. Malek *et al.* [Pierre Auger Collaboration], *Proc. 29th ICRC*, Pune, **8**, 335 (2005).
 31. F. Nerling *et al.* [Pierre Auger Collaboration], *Proc. 29th ICRC*, Pune, **7**, 127 (2005), [arXiv:astro-ph/0507251]; M. Unger, in preparation (2006).
 32. T.K. Gaisser, A.M. Hillas, *Proc. 15th ICRC*, Plovdiv, **8**, 353 (1977)
 33. T. Pierog *et al.*, *Proc. 29th ICRC*, Pune, **7**, 103 (2005).
 34. T. Bergmann *et al.*, *Astropart. Phys.*, in print (2006), [arXiv:astro-ph/0606564].
 35. L. Prado *et al.*, *Nucl. Instr. Meth.* **A545**, 632 (2005).
 36. T.C. Rogers, M.I. Strikman, *J. Phys. G: Nucl. Part. Phys.* **32**, 2041 (2006)
 37. M. Risse *et al.*, *Czech. J. Phys.* **56**, A327 (2006) [arXiv:astro-ph/0512434].
 38. K. Shinozaki *et al.*, *Astrophys. J.* **571**, L117 (2002).
 39. M. Risse *et al.*, *Phys. Rev. Lett.* **95**, 171102 (2005).
 40. M. Ave *et al.*, *Phys. Rev. Lett.* **85**, 2244 (2000); *Phys. Rev.* **D65**, 063007 (2002).
 41. X. Bertou, P. Billoir, S. Dagoret-Campagne, *Astropart. Phys.* **14**, 121 (2000).
 42. P. Homola *et al.*, *Characteristics of geomagnetic cascading of ultra-high energy photons at the southern and northern sites of the Pierre Auger Observatory*, *Astropart. Phys.* (2006), in press, doi:10.1016/j.astropartphys.2006.10.005, [arXiv:astro-ph/0608101].